1967, *Bull. Astr. Inst. Netherlands* **19** 254–259; *Communication from the Observatory at Utrecht*

CORONAL SCATTERING OF RADIATION FROM AN ANISOTROPICALLY RADIATING SOLAR RADIO SOURCE

A. D. FOKKER and R. J. RUTTEN

Received 14 June 1967

As shown by FOKKER (1965) it is possible to simulate coronal scattering of solar radio sources with a ray tracing technique in which the paths of many rays through the corona are computed, scattering being accounted for with a randomly deflecting procedure. In this paper we describe an extension of this computing program to the general case in which the source is not necessarily isotropical. As a testing case we discuss the effects of coronal scattering on a source which radiates only in a narrow cone, off-set from the radius vector by 45°. Results are given for different positions of the source on the solar disk.

1. Introduction

Due to coronal scattering the angular diameter of a radio source appears enlarged when seen through the solar corona; obviously the same process deforms solar radio sources as well. Whereas the observations of the angular extent of solar radio bursts give results in the order of a few minutes of arc (HÖGBOM, 1959: 6′ at 81 Mc/s; FOKKER, 1960: 3′ at 200 Mc/s), the actual sources might be much smaller; in general, coronal scattering may introduce also displacements of source positions and asymmetries in the brightness distributions.

FOKKER (1965) showed the possibility of studying scatter images by model computations in which a great number of rays, emerging in different directions from a point source, are traced throughout a scattering spherical corona. In this procedure the finally outcoming rays are taken together in groups according to their final direction; each group defines a different position of the source on the solar disk. Scattering is introduced by giving each ray a number of discrete deflections; the magnitude of each deflection is chosen at random from a Gaussian distribution. The path length between two successive deflections is chosen proportional to r/N^2, with the coronal density $N(r)$ taken from an appropriate coronal model (r = distance to the solar centre in units $R_\odot$). Finally the apparent position on the solar disk is plotted for each ray belonging to a particular group along with the true position of the point source for that group on the disk: the result is a scatter diagram which outlines the apparent source. The characteristics as displacement, size and shape of the scatter image are determined statistically.

In this manner FOKKER (1965; hereafter referred to as Paper I) determined the scatter images for different positions on the disk of a source radiating isotropically without any directivity within a wide cone (156° aperture) with the radius vector as axis.

This paper presents an extension of Paper I: by exactly the same procedure we obtain scatter images for sources radiating with substantial directivity in an oblique direction. The radiation is taken to be confined to a narrow cone (40° aperture) with an axis off-set 45° from the radius vector; the source is taken at a height of 0.3 $R_\odot$ above the photosphere.

The reason for investigating this case is the fact, established from observations, that the position of the source of storm radiation may deviate appreciably from the position of the sunspot group with which the noise storm is associated, even for positions near the centre of the solar disk. LE SQUEREN-MALINGE (1963) found that the deviations between the positions of sunspots and the associated radio storm centres are of the order of a few minutes of arc. To some extent such deviations might be due to the radiation of the source being emitted in an oblique direction. Even if the source is situated right over the sunspot, the scatter image in

that case would be formed at a place some distance apart from the sunspot. It is to this question that we wish to apply our technique of ray tracing.

2. Computations

As in Paper I, we adopted a spherical corona with densities according to the Newkirk model. In the model for the scattering process we adopted the same distribution of deflection angles and the same numerical relation for path lengths between successive deflections as a function of the distance to the solar centre.

The direction of emission of an individual ray can be specified by two angles: the angle α between the ray and the normal and the azimuth angle β. When the cone has the radius vector as axis, all rays with the same α are equivalent; they may therefore be grouped. In the present case the rays must be divided in groups according to both α and β.

We approximated the radiating cone by covering it with 21 pairs of (α, β) combinations (see figure 1); for each initial direction (α, β) we computed 100 rays on the Electrologica X-8 computer of the Computing Centre of the University of Utrecht.

When each ray passed the 1.6 $R_\odot$ level, scattering was stopped and the ray was presumed to travel along a rectilinear path to the Earth; this final direction (α_0, β_0) defines the position of the point source S on the solar disk: for $\alpha_0 = 0°$ S is in the centre of the disk, for $\alpha_0 = 90°$ on the limb, the position angle being given by β_0. We divided the possible (α_0, β_0) combinations in 25 groups; each group is contained in a field comprising ranges of 30° in α_0 and β_0. All rays with α_0 and β_0 in the same group were taken together. The apparent origin of each ray was computed in a plane through S perpendicular to the axis of the field. The extended final ray intersects this place at S′ and the projection of the Sun's centre on this plane is C′. The length of SS′ and the position angle C′SS′ were computed. The latter angle had to be computed in the full range of 2π radians since the scatter image cannot a priori be expected to be symmetrical.

By plotting all apparent source positions for a given field together in a polar plot, we obtain the scatter image of the source; the position of the source on the solar disk is given by the direction of the axis of the field in question.

2.1. *Discussion*

Each field having a limited size, the scatter image composed by rays that belong to a given field can be considered as representative for the position of a source on the Sun's disk that corresponds with the axis of the field.

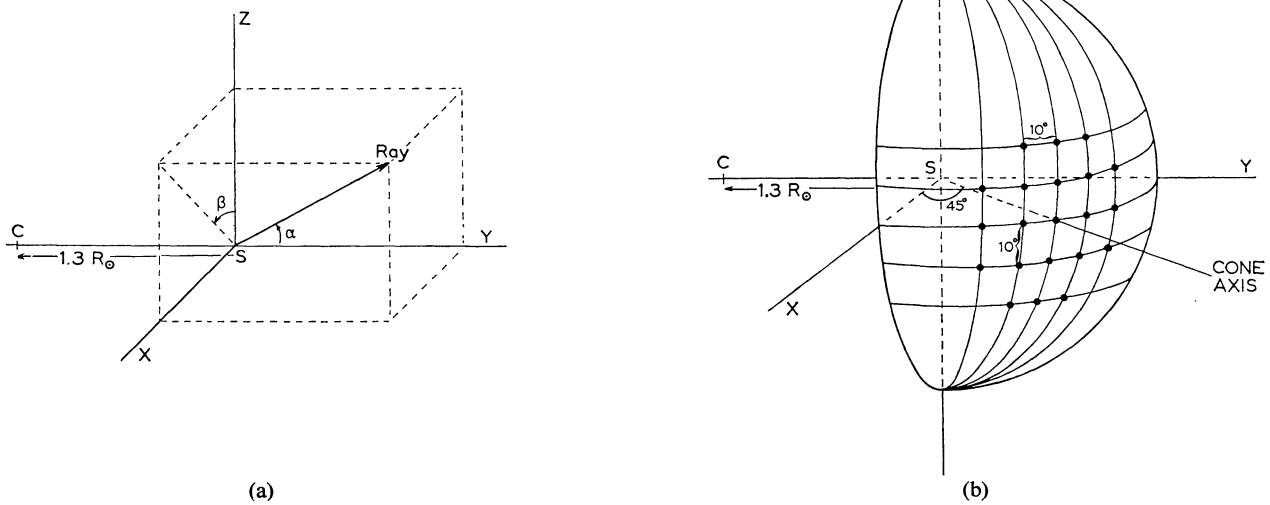

Figure 1. In figure 1a the definition of the used polar coordinates is given. C: Solar centre; S: Point source at 1.3 $R_\odot$. The direction of the axis of the radiating cone is: $\alpha = 45°$, $\beta = 90°$. In figure 1b we show the used approximation for a radiating cone with a 40° aperture and a 45° tilt. In each direction (black dot) we computed 100 rays.

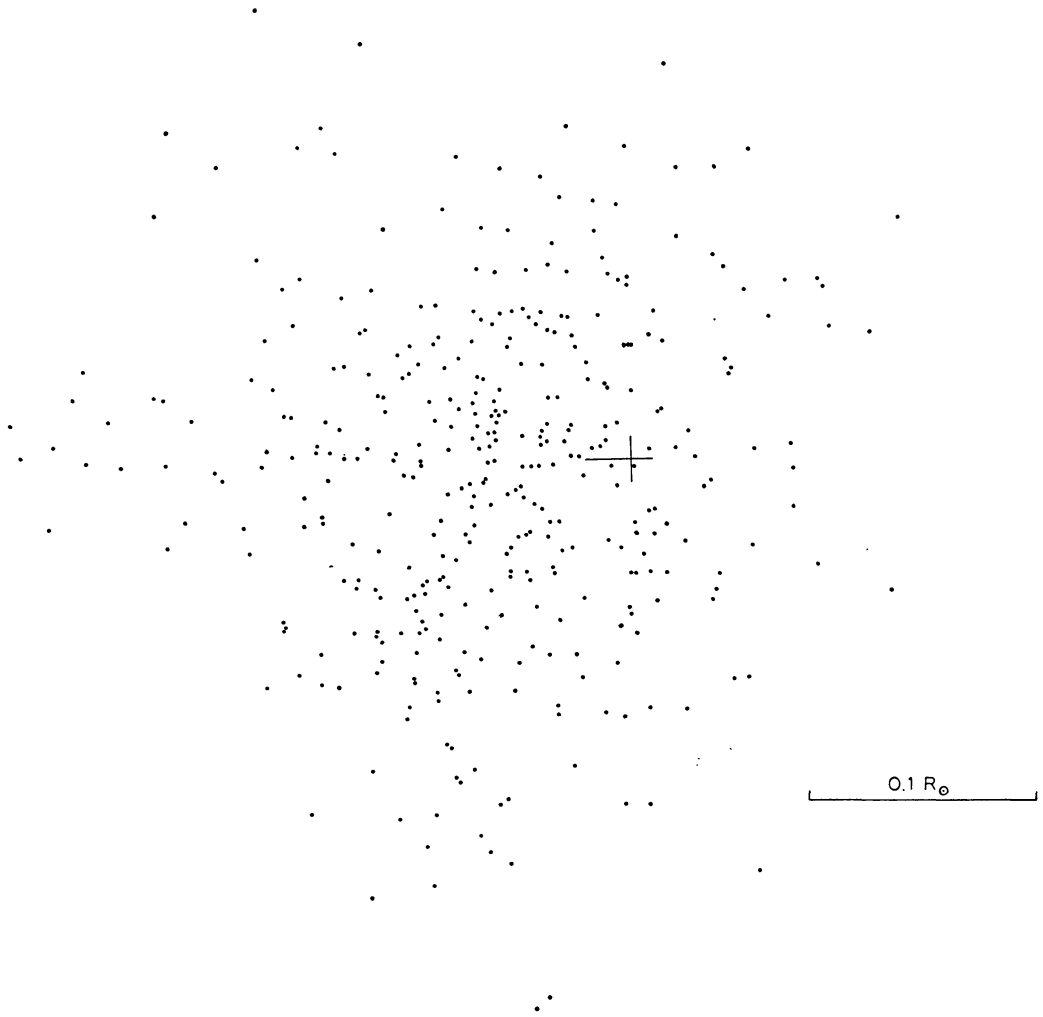

Figure 2. Scatter image for a source near the solar centre. The true source position is given by the cross; the projected direction of the source axis is to the left.

Unlike the procedure adopted in Paper I, where the configuration C′SS′ was computed for a plane perpendicular to the direction of the ray itself, we took in the present case a common plane through S perpendicular to the field axis. It proved advantageous to do so for those rays that belong to the field corresponding to $\alpha_0 = 0°$ (the central field, case 2 of figure 4) for the reason that in the central field the scatter image is not symmetrical around S, unlike the case in Paper I.

For the sake of convenience, a common plane, perpendicular to the field axis, was also adopted for rays that belong to non-central fields. For a number of rays we compared the results of the two procedures (i.e., taking a common plane and taking planes perpendicular to each individual ray); the mean error in position of S′ equals 0.001 $R_\odot$, which we consider sufficiently small.

We did not take into account the well-known continuous bending of rays in a smooth corona for reasons given in Paper I.

3. Results

Figure 2 shows as example the scatter diagram obtained for a source near the solar centre (all rays with $\alpha_0 < 30°$). We determined the intensity distribution by counting points in strips parallel and perpendicular to the projected axis of the radiation cone, respectively. The

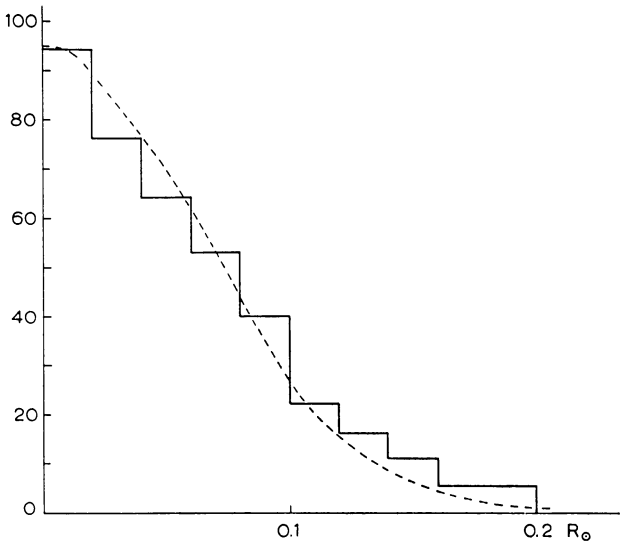

Figure 3. The intensity distribution for a source in the solar centre, perpendicular to the projected source axis. The dashed line is a Gaussian distribution.

first distribution appears to be close to a Gaussian distribution (see figure 3); the other one, along a direction parallel to the projected cone axis, is given in figure 4.

Similar diagrams were obtained for other source positions. In figure 4 we show intensity distributions for four different source positions, all with the axis of the radiation cone in the plane through the observer's direction and the radius vector through S (henceforward this plane is called "the reference plane").

Figure 5 illustrates a case ("case 5") in which the cone axis points away from the reference plane; the coordinates of the axis of the field are: $\alpha_0 = 75°$, $\beta_0 = 0°$. As expected, the displacement of the scatter image from the source position has components both parallel and perpendicular to the projected radius vector. The displacements in these directions are about equal. The results for the different cases are collected in table 1. We note the following points.

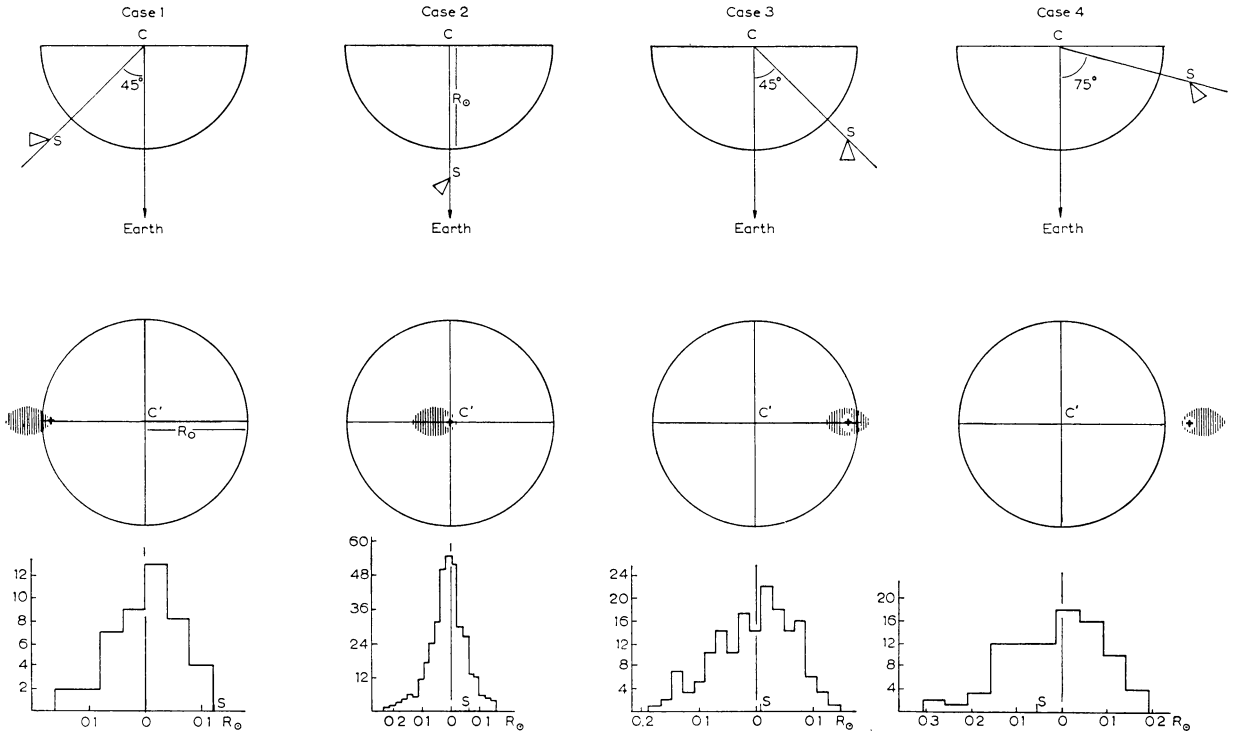

Figure 4. Intensity distributions for sources with the cone axis in the plane through the observer's direction and the radius vector through S. The vertical columns present four different source positions (cases 1 to 4). The top row gives for each case the source position and direction in the reference plane; the second row shows the solar disk as seen from the Earth. The shaded area represents the scatter image (exaggerated) and the cross the true position S. The bottom row shows the intensity distribution parallel to C'S; the central line corresponds with the centre of gravity and S denotes the true source position.

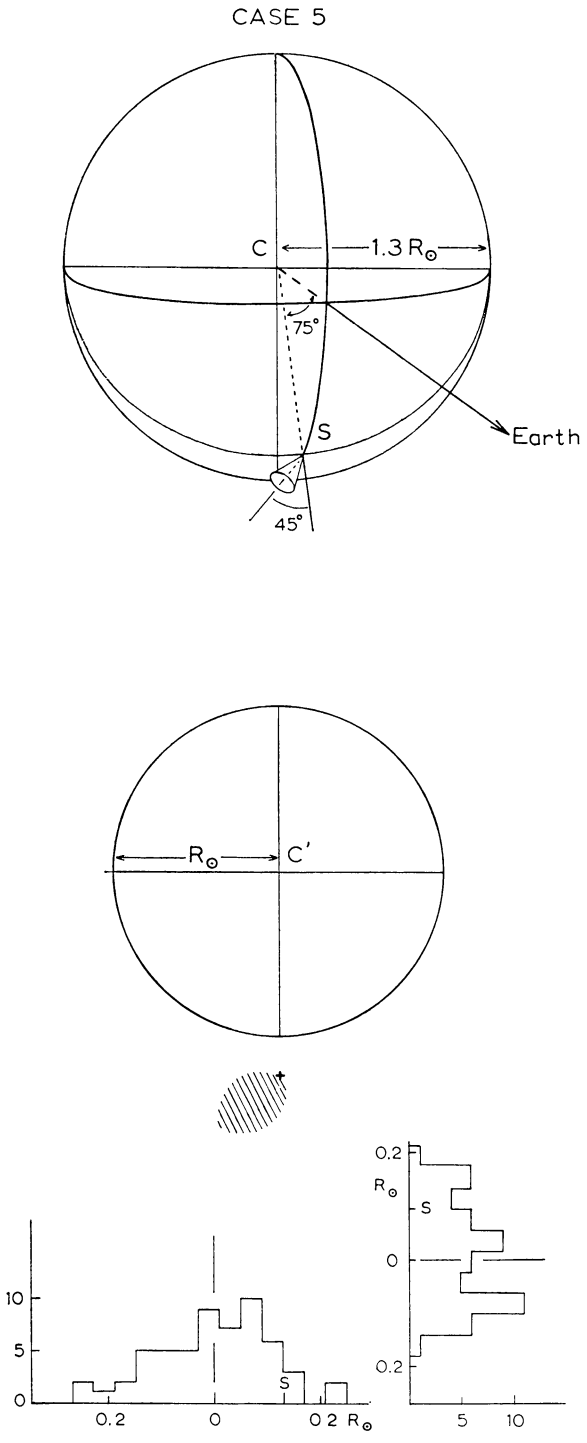

Figure 5. Intensity distribution for a source pointing away from the reference plane. From top to bottom: the position and direction of the source, the apparent solar disk and the vertical and horizontal intensity distribution.

a) *Diameters*

As diameter we define the distance between the points in the scatter image where the intensity is reduced to $1/e$ of the top value. We find an increase of the diameter from centre to limb from about 2′ to about 5′. Sizes like this agree with the existing observational evidence.

b) *Displacements*

As position of the apparent source we take the position of the centre of gravity of the scatter image. This position is displaced from the true source position in an obvious way. As expected, the displacement for the cases 3 and 4 (see figure 4) are smaller than in the corresponding cases treated in Paper I (an isotropically radiating source at the limb is seen displaced over 0.10 $R_\odot$), but the displacement in case 1 is appreciably larger than for a corresponding isotropically radiating source.

c) *Asymmetries*

As in Paper I, the asymmetry a of the scatter image is defined as $a = |(r-l)|/(r+l)$, where r and l denote the numbers of points to the right and to the left of the centre of gravity. Except for case 1, the asymmetries are smaller than those found for an isotropically radiating source (paper I: $a = 0.15$ at the limb and $a = 0.10$ at a position intermediate between cases 3 and 4).

d) *Intensities*

The intensity in a particular direction is proportional to the number of rays per solid angle. In table 1 are given the relative intensities as derived from the number of dots contained in a field.

4. Conclusion

For Earth directions not too different from the direction of the radiating cone's axis (cases 2 to 4) we find similar scatter images as in Paper I. When the observer's direction is quite different from the cone's axis, the relative intensity is small but the displacements and asymmetries are bigger.

We conclude that the various deviations of source positions from the positions of the corresponding optical centres, as observed by Le Squeren-Malinge, need not be fully due to different heights of the sources or

TABLE 1

	Case 1 ($\alpha_0 = 45°$; $\beta_0 = 270°$)	Case 2 ($\alpha_0 = 0°$)	Case 3 ($\alpha_0 = 45°$; $\beta_0 = 90°$)	Case 4 ($\alpha_0 = 75°$; $\beta_0 = 90°$)	Case 5 ($\alpha_0 = 75°$; $\beta_0 = 0°$)
Number of rays	45	399	163	83	56
Diameter to $1/e$ of top value	0.19 $R_\odot$	0.16 $R_\odot$	0.20 $R_\odot$	0.30 $R_\odot$	0.25 $R_\odot$
Displacement	0.12 $R_\odot$	0.07 $R_\odot$	0.0	0.06 $R_\odot$	0.17 $R_\odot$
Asymmetry a	0.11	0.0	0.07	0.06	0.09
Relative intensity	1	6	10	4	1

to the fact that they are not situated radially above the optical centre. On top of these possible causes of positional differences may come shifts in positions of the order of 1′–2′ for radiation that is emitted in oblique directions, making angles with the radius vector of the order of 45°.

In this work we have rather arbitrarily chosen a 40°-cone off-set over 45° as radiating source; however, the computing program is kept quite general and it will be easy to compute scatter images for any type of directional cone and also for different scattering efficiencies when the need arises.

Acknowledgements

We thank Mr. G. W. Geijtenbeek for much help in the development of the computing program. We are also indebted to the staff of the Computing Centre of Utrecht University for allotting the necessary computing time.

References

A. D. FOKKER, 1960, Thesis, Leiden University
A. D. FOKKER, 1965, *Bull. Astr. Inst. Netherlands* **18** 111
J. A. HÖGBOM, 1959, Thesis, Cambridge University
A. M. LE SQUEREN-MALINGE, 1963, *Ann. Ap.* **26** 97